International Journal of Pharmaceutics 531 (2017) 550–558

Contents lists available at ScienceDirect

International Journal of Pharmaceutics

journal homepage: www.elsevier.com/locate/ijpharm

Polymer-free electrospun nanofibers from sulfobutyl ether$_7$-beta-cyclodextrin (SBE$_7$-β-CD) inclusion complex with sulfisoxazole: Fast-dissolving and enhanced water-solubility of sulfisoxazole

Zehra Irem Yildiz, Asli Celebioglu, Tamer Uyar*

Institute of Materials Science & Nanotechnology, UNAM-National Nanotechnology Research Center, Bilkent University, Ankara 06800, Turkey

ARTICLE INFO

Article history:
Received 27 February 2017
Received in revised form 13 April 2017
Accepted 20 April 2017
Available online 23 April 2017

Keywords:
Electrospinning
Electrospun nanofibers
Sulfobutyl ether$_7$-beta-cyclodextrin (Captisol®)
Sulfisoxazole
Inclusion complex
Water-Solubility

ABSTRACT

In this study, our aim was to develop solid drug-cyclodextrin inclusion complex system having nanofibrous morphology in order to have fast-dissolving property and enhanced water-solubility of poorly water-soluble drug. Here, we prepared a highly concentrated aqueous solution of inclusion complex between sulfisoxazole and sulfobutyl ether$_7$-beta-cyclodextrin (SBE$_7$-β-CD, Captisol®), and then, without using any polymeric matrix, the electrospinning of sulfisoxazole/SBE$_7$-β-CD-IC nanofibers was performed in order to obtain free-standing and handy nanofibrous web. As a control sample, nanofibers from pure SBE$_7$-β-CD was also electrospun and free-standing nanofibrous web was obtained. The SEM imaging revealed that the bead-free and uniform nanofiber morphology with the average fiber diameter (AFD) of 650 ± 290 nm for sulfisoxazole/SBE$_7$-β-CD-IC NF and 890 ± 415 nm for pure SBE$_7$-β-CD NF was obtained. The inclusion complex formation between sulfisoxazole and SBE$_7$-β-CD in sulfisoxazole/SBE$_7$-β-CD-IC NF sample was confirmed by ^{1}H NMR, TGA, DSC, XRD and FTIR analyses. Due to the combined advantage of cyclodextrin inclusion complexation and high surface area of electrospun nanofibers, fast-dissolving property with enhanced water-solubility was successfully achieved for sulfisoxazole/SBE$_7$-β-CD-IC NF. Our findings suggest that electrospun nanofibers/nanowebs from CD-IC of poorly water-soluble drugs may offer applicable approaches for high water-solubility and fast-dissolving tablet formulations for drug delivery systems.

1. Introduction

Cyclodextrins (CDs) are cyclic oligosaccharides having either 6, 7, or 8 glucopyranose units linked by α-1,4 linkages in the cycle and are named as α-CD, β-CD and γ-CD, respectively (Szejtli, 1998). CDs have truncated cone-shaped molecular structure which can form supramolecular structures by forming non-covalent host-guest inclusion complexes with variety of molecules (Szejtli, 1998). The inner side of the CD is relatively hydrophobic and the outer side is hydrophilic which makes CDs to form inclusion complexes with various hydrophobic molecules including drug molecules (Ogawa et al., 2015). One of the main problems in pharmaceutical industry is low water-solubility of the drugs which result in decrease in bioavailability; nevertheless, the inclusion complex formation of drugs with cyclodextrins overcomes this problem and enhances the bioavailability of the drugs by increasing their water-solubility. But, native cyclodextrins (α-CD, β-CD and γ-CD) have lower water-solubility which sometimes restricted their use in pharmaceutical formulation. Yet, chemically modified CD derivatives such as hydroxypropyl-CD, methylated-CD, sulfobutyl ether-CD have much higher water solubility. Sulfobutyl ether-beta-cyclodextrin (SBE$_7$-β-CD, Captisol®) is sulfobutyl derivative of β-CD with a 6.6 average degree of substitution (Fig. 1a). This substitution decreases nephrotoxicity of cyclodextrin while increases its aqueous solubility to a great extent (Beig et al., 2015). One of the distinctive features of SBE$_7$-β-CD is extension of the cavity due to repulsion of end groups' negative charges which provides stronger binding to the drug molecules (Beig et al., 2015). The other feature is the presence of negative charges in SBE$_7$-β-CD at physiological pH which makes binding with a positively charged drug molecule possible. Therefore, the inclusion complex formation with SBE$_7$-β-CD has advantages for drug delivery systems.

The application of inclusion complexes of CDs with drug may be widen by the incorporation of such molecular complexation

* Corresponding author.
E-mail addresses: tamer@unam.bilkent.edu.tr, tameruyar@gmail.com (T. Uyar).

http://dx.doi.org/10.1016/j.ijpharm.2017.04.047
0378-5173/

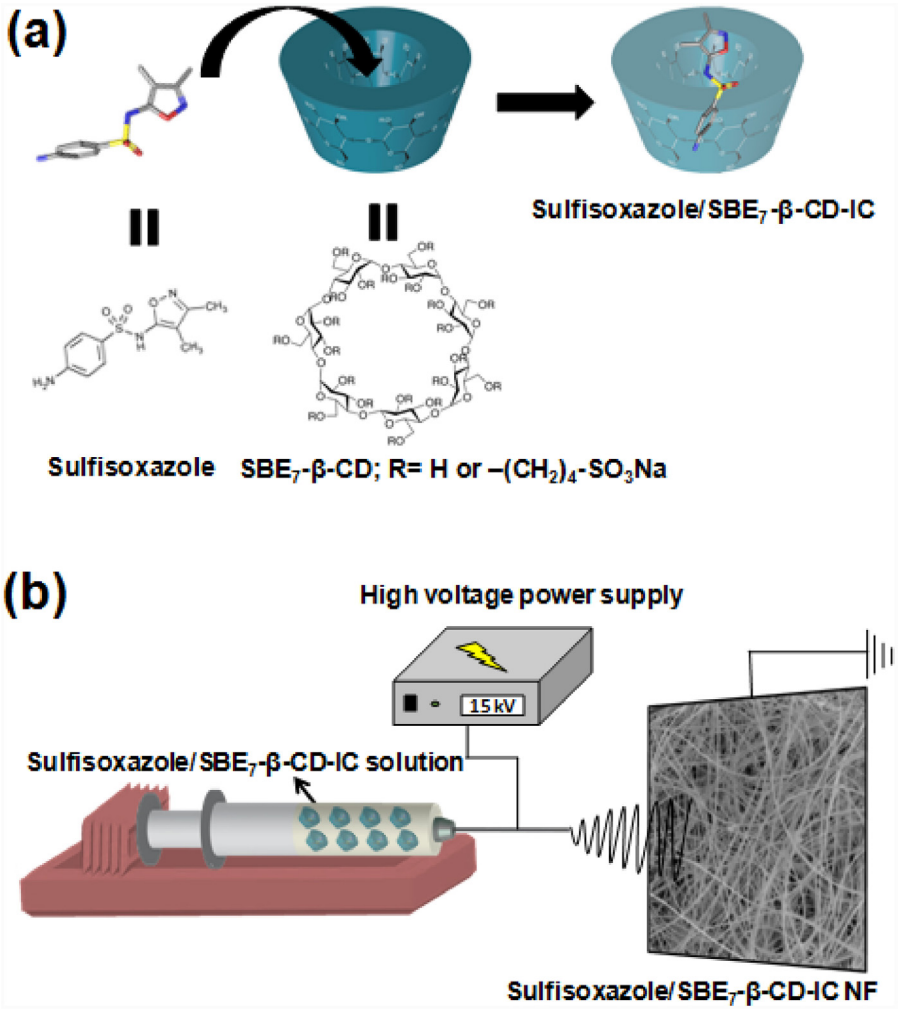

Fig. 1. **(a)** The chemical structure of sulfisoxazole and SBE_7-β-CD with a schematic representation of sulfisoxazole, SBE_7-β-CD and their IC, **(b)** Schematic representation of the electrospinning of sulfisoxazole/SBE_7-β-CD-IC NF.

systems into highly porous nanofibrous carrier matrix. Electrospinning, being one of the versatile methods for nanofiber production, enables us to produce nanofibers and nanofibrous webs having high surface area to volume ratio, nano-scale porosity and design flexibility for chemical/physical functionalization, etc. Due to their exceptional properties, it has been shown that electrospun nanofibers and their nanomats/nanowebs have potential use in various application areas in biotechnology, membranes/filters, food, agriculture, sensor, energy etc, (Aytac et al., 2015, 2017; Noruzi, 2016; Sahay et al., 2012; Uyar and Kny, 2017). Electrospun nanofibers could also be used for drug delivery systems for targeted delivery and/or for inhibition of drug adverse side effects with controlled release (Aytac et al., 2015; Mendes et al., 2016; Wang et al., 2016).

Electrospun polymeric nanofibers incorporating drug-cyclodextrin inclusion complexes (CD-ICs) have shown to be promising matrix for drug release systems (Aytac et al., 2015; Aytac and Uyar, 2017; Tonglairoum et al., 2013). For instance, Siafaka et al. (2016) has performed a study on the comparison of electrospun nanofibers and cyclodextrin as drug delivery system suggesting that both systems were good for drug delivery and showed similar efficiency. In our approach, we combine the efficiency of cyclodextrin inclusion complexation and high surface area of electrospun nanofibers for effective drug delivery system. Since electrospinning of nanofibers from small molecules is quite a challenge, mostly polymeric matrix is needed to obtain nanofibers (Uyar and Kny, 2017; Wendorff et al., 2012). Nevertheless, in our recent studies we achieved the electrospinning of nanofibers from pure cyclodextrin types (native CDs and modified CDs) (Celebioglu and Uyar, 2012, 2013; Celebioglu et al., 2014b) and CD-ICs (Celebioglu and Uyar, 2011; Celebioglu et al., 2014a, 2016; Aytac et al., 2016a,b) without using polymeric carrier matrix.

Sulfonamides are synthetic drugs known by their antimicrobial effects on different pathogenic microorganisms (Tačić et al., 2014). However, the use of these types of drugs is sometimes limited due to their poor water-solubility. The oxazole subtituted sulfonamide is called as sulfisoxazole (Fig. 1a). Sulfisoxazole is a weak acid and slightly soluble in water. In this study, our aim was to develop nanofibrous sulfisoxazole-cyclodextrin inclusion complex system (Fig. 1a) in order to have fast-dissolving character and enhance the water-solubility of sulfisoxazole. Here, we prepared a highly concentrated aqueous solution of inclusion complex between sulfisoxazole and SBE_7-β-CD, and then, without using any polymeric matrix, sulfisoxazole/SBE_7-β-CD-IC was electrospun into nanofibrous structure to obtain a free-standing and handy solid form (Fig. 1b). We observed that sulfisoxazole/SBE_7-β-CD-IC nanofibrous web was readily soluble in water and the water-solubility of sulfisoxazole was enhanced significantly. Our findings

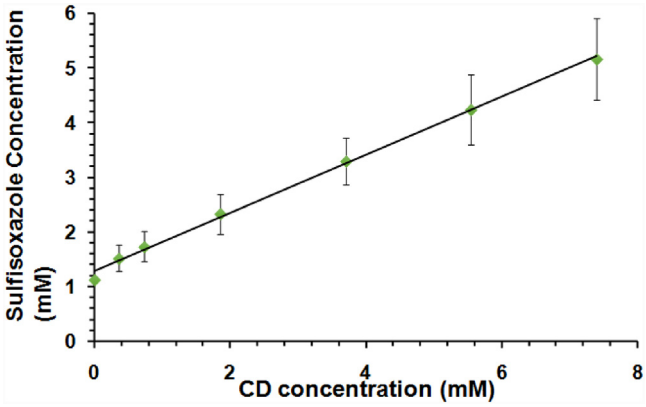

Fig. 2. Phase solubility diagram of sulfisoxazole/SBE_7-β-CD systems in water (n = 3).

suggested that sulfisoxazole/SBE_7-β-CD-IC in the form of nanofibrous webs can be quite useful in fast-dissolving tablet formulations for drug delivery.

2. Materials and methods

Sulfisoxazole (99%) was obtained from Sigma-Aldrich commercially. SBE_7-β-CD (Captisol®, average degree of substitution = 6.6) was kindly donated by Cydex Pharmaceuticals Inc. (Kansas, USA). Potassium bromide (KBr, 99%, FTIR grade, Sigma-Aldrich), deuterated dimethylsulfoxide (d6-DMSO, deuteration degree min. 99.8% for NMR spectroscopy, Merck) were used in this study. The water used was from a Millipore Milli-Q ultrapure water system. The materials were used as-received without any further purification process.

2.1. Preparation of solutions

The inclusion complex solution of sulfisoxazole with SBE_7-β-CD was initially prepared by 1:1 molar ratio of sulfisoxazole:SBE_7-β-CD. However, the molar ratio was changed to 1:2 (sulfisoxazole:SBE_7-β-CD) since electrospinning of uniform nanofiber cannot be obtained from 1:1 complex solution. Firstly, sulfisoxazole powder was dispersed in water then SBE_7-β-CD (200% (w/v)) was added to the dispersion. After that, the solution was stirred 24 h until clear and homogenous solution was obtained. Besides, to make comparison, highly concentrated SBE_7-β-CD (200% (w/v)) solution without sulfisoxazole was also prepared in water for the electrospinning of pure SBE_7-β-CD nanofibers. Sulfisoxazole/SBE_7-β-CD-IC was also obtained in the powder form in order to compare with sulfisoxazole/SBE_7-β-CD-IC NF in terms of the dissolving rate and water solubility. Sulfisoxazole powder was dispersed in water and then SBE_7-β-CD was added with the molar ratio of 1:2 (sulfisoxazole:SBE_7-β-CD). After 24 h stirring, this inclusion complex solution was frozen at −80 °C for two days and then lyophilized in a freeze-dryer for 24 h to obtain sulfisoxazole/SBE_7-β-CD-IC powder.

2.2. Electrospinning of nanofibers

Sulfisoxazole/SBE_7-β-CD-IC solution was loaded to the 1 mL syringe fitted with a 0.4 mm inner diameter having needle. The syringe was placed horizontally on the syringe pump (KD Scientific, KDS 101) and the solution was pumped with rate of

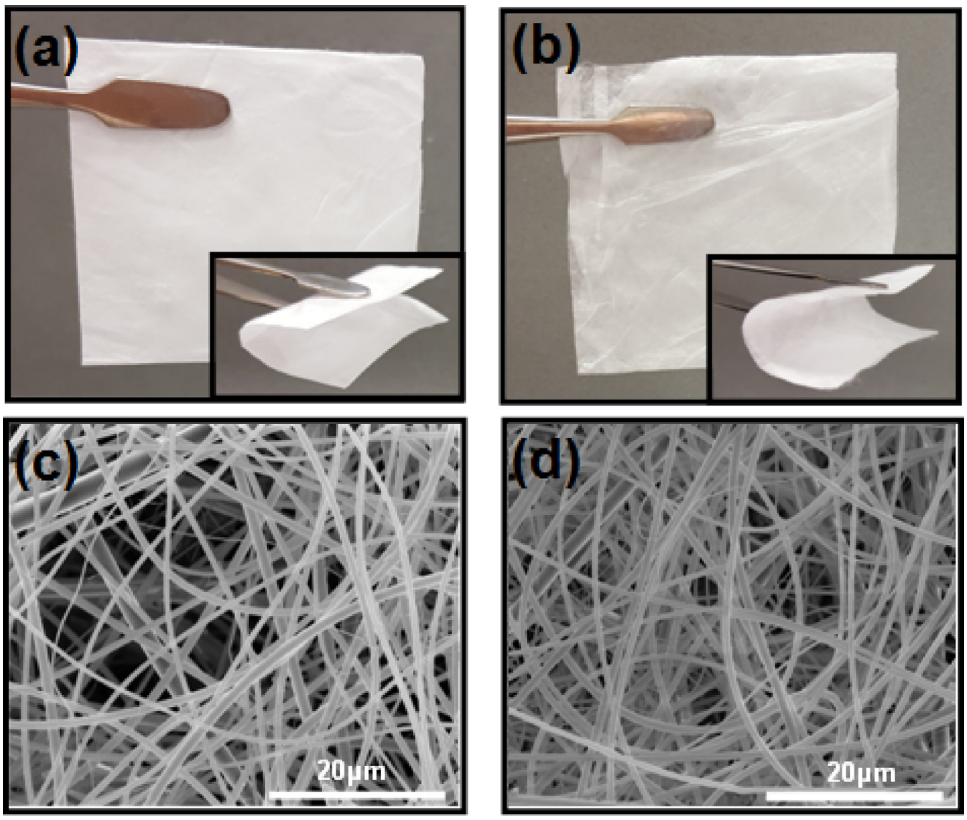

Fig. 3. Photographs of electrospun **(a)** SBE_7-β-CD NF, **(b)** sulfisoxazole/SBE_7-β-CD-IC NF, and SEM images of **(c)** SBE_7-β-CD NF, **(d)** sulfisoxazole/SBE_7-β-CD-IC NF.

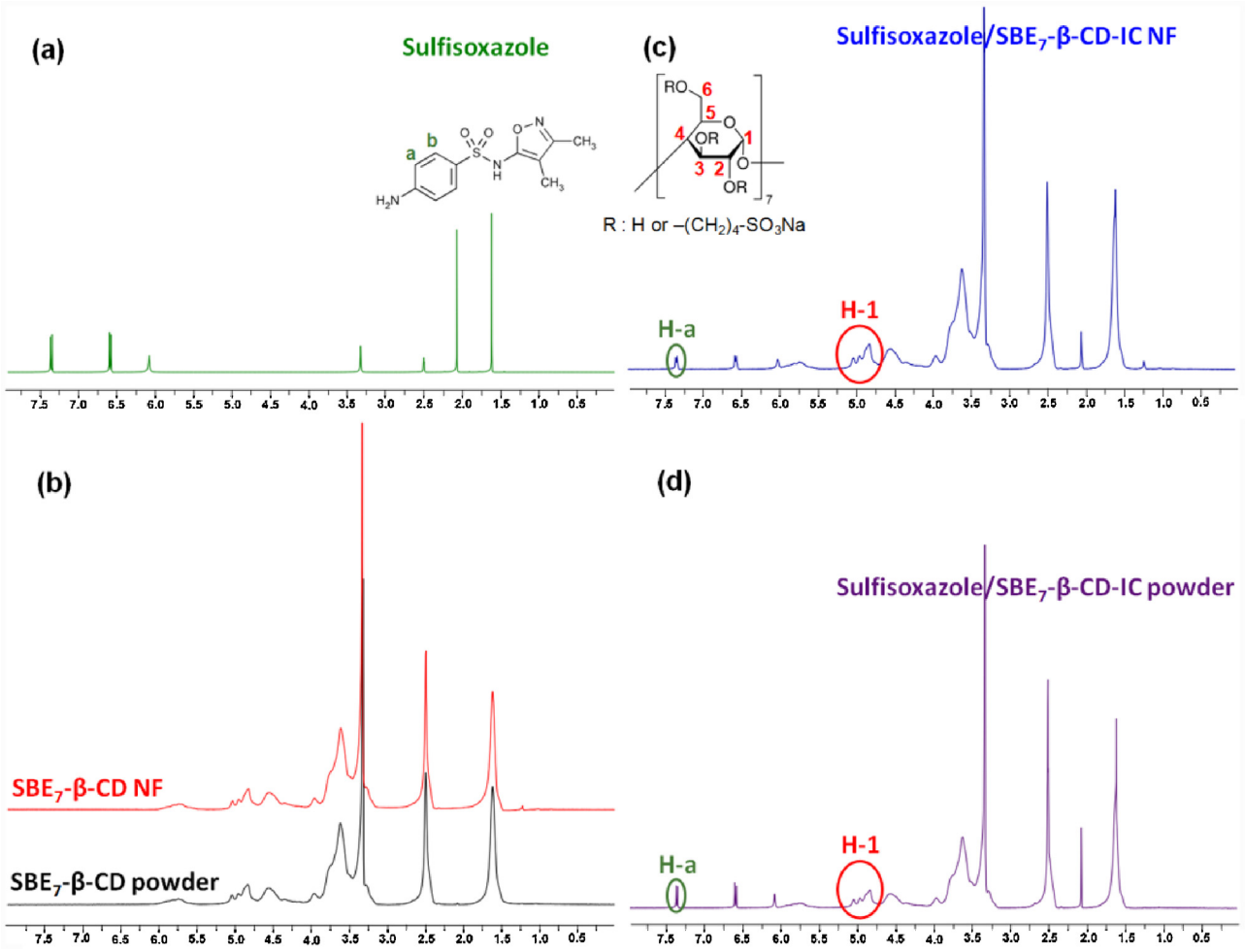

Fig. 4. ^{1}H NMR spectra of **(a)** sulfisoxazole powder, **(b)** SBE_7-β-CD NF and SBE_7-β-CD powder, **(c)** sulfisoxazole/SBE_7-β-CD-IC NF, **(d)** sulfisoxazole/SBE_7-β-CD-IC powder.

0.5–1 mL/h. A grounded metal collector covered by aluminum foil was placed at 10–15 cm from the tip of the needle and the applied voltage was 10–15 kV. The electrospinning of pristine SBE_7-β-CD NF was performed with the same conditions/parameters. The electrospinning system was enclosed by Plexiglass box and electrospinning was performed at 25 °C and 30% relative humidity.

2.3. Measurements and characterizations

Phase solubility measurement was carried out according to Higuchi and Connors (1965). An excess amount of sulfisoxazole was added to 5 mL of aqueous solutions containing increasing concentration of SBE_7-β-CD ranging from 0 to 7.4 mM. The

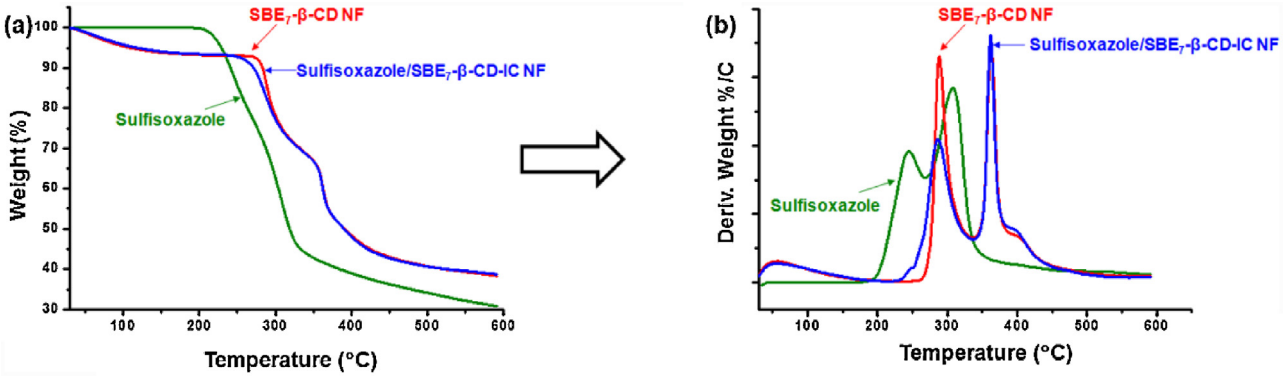

Fig. 5. **(a)** TGA thermograms and **(b)** their derivatives of sulfisoxazole, SBE_7-β-CD NF and sulfisoxazole/SBE_7-β-CD-IC NF.

suspensions were shaken for 48 h at room temperature to reach equilibrium. Then, all suspensions were filtered by a 0.45 μm membrane filter to remove undissolved parts and all suspensions were diluted with water. Sulfisoxazole concentration with respect to increasing SBE_7-β-CD concentration was determined by UV–vis spectroscopy (Varian, Cary 100) at 260 nm. The result of phase solubility was given as a plot of the molar concentration of sulfisoxazole versus molar concentration of SBE_7-β-CD. The apparent stability constant (K_s) of sulfisoxazole/SBE_7-β-CD-IC were calculated from the phase solubility diagram according to the following equation:

$$K_s = \text{slope}/S_0\ (1\text{-slope}) \quad (1)$$

where S_0 is the intrinsic solubility of sulfisoxazole.

The samples of electrospun nanofibers (SBE_7-β-CD NF and sulfisoxazole/SBE_7-β-CD-IC NF) were investigated morphologically by scanning electron microscopy (SEM, FEI-Quanta 200 FEG). Nanofibers were sputtered with 5 nm Au/Pd layer to minimize charging by PECS-682. Average fiber diameter (AFD) for both nanofibrous web was calculated from SEM images of 100 fibers.

The proton nuclear magnetic resonance (^{1}H NMR, Bruker D PX-400) system was used to determine molar ratio between sulfisoxazole and SBE_7-β-CD. In addition, SBE_7-β-CD powder was also analyzed by ^{1}H NMR to see if there is any change due to degradation in chemical structure of SBE_7-β-CD after electrospinning process. 30 g L^{-1} concentration of pure sulfisoxazole, SBE_7-β-CD powder, SBE_7-β-CD NF, sulfisoxazole/SBE_7-β-CD-IC NF and sulfisoxazole/SBE_7-β-CD-IC powder was dissolved in d6-DMSO separately for the preparation of solution for ^{1}H NMR measurements.

Thermogravimetric analysis (TGA, TA Q500, USA) was carried out to determine the thermal properties of sulfisoxazole, SBE_7-β-CD NF and sulfisoxazole/SBE_7-β-CD-IC NF. These studies of the samples were performed from 25 to 600 °C with a heating rate of 20 °C/min under nitrogen gas flow.

Differential scanning calorimetry (DSC, TA Q2000, USA) was used to analyze inclusion complex formation between sulfisoxazole and SBE_7-β-CD. DSC measurement was performed for sulfisoxazole, SBE_7-β-CD NF, sulfisoxazole/SBE_7-β-CD-IC NF and sulfisoxazole/SBE_7-β-CD-IC powder under N_2. Samples were equilibrated at 50 °C and heated to 220 °C with a rate of 10 °C/min.

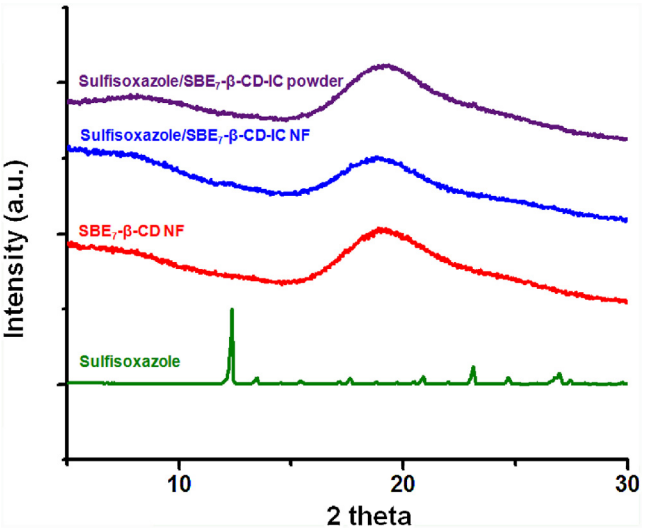

Fig. 7. XRD patterns of sulfisoxazole, SBE_7-β-CD NF sulfisoxazole/SBE_7-β-CD-IC NF and sulfisoxazole/SBE_7-β-CD-IC powder.

X-ray diffraction (XRD) (PANalytical X'Pert powder diffractometer) measurements of pure sulfisoxazole, SBE_7-β-CD NF, sulfisoxazole/SBE_7-β-CD-IC NF and sulfisoxazole/SBE_7-β-CD-IC powder were recorded by applying Cu Kα radiation in a range of 2θ = 5–30° to determine the crystalline structure of the samples.

Fourier transform infrared spectrometry (FTIR, Bruker-VERTEX70) was used to obtain the infrared spectra of the samples. The samples were mixed with potassium bromide (KBr) and pressed as pellets. 64 scans were recorded between 4000 and 400 cm^{-1} at a resolution of 4 cm^{-1}.

The water solubility of sulfisoxazole is quite limited (Gladys et al., 2003). Here, excess amount of sulfisoxazole (1.3 mg mL^{-1}), and sulfisoxazole/SBE_7-β-CD-IC NF and sulfisoxazole/SBE_7-β-CD-IC powder having the same amount of sulfisoxazole were added to the water and stirred overnight. To make comparison, the solution of sulfisoxazole with concentration of its water solubility (about 0.2 mg mL^{-1}) was also prepared and stirred overnight. After that, all samples were filtered through a 0.45 μm membrane filter to

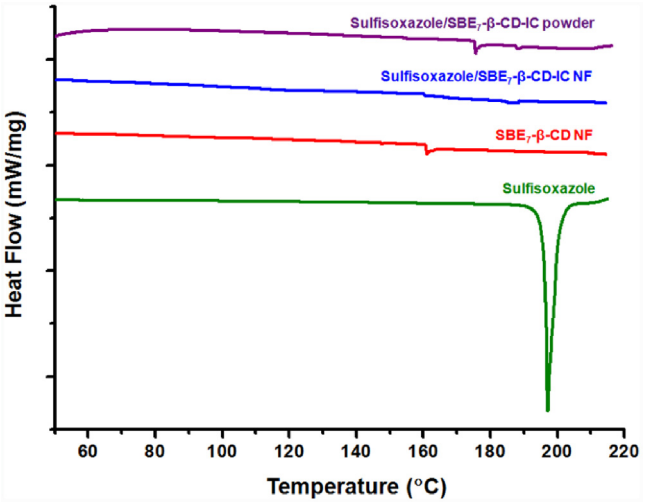

Fig. 6. DSC thermogram of sulfisoxazole, SBE_7-β-CD NF, sulfisoxazole/SBE_7-β-CD-IC NF and sulfisoxazole/SBE_7-β-CD-IC powder.

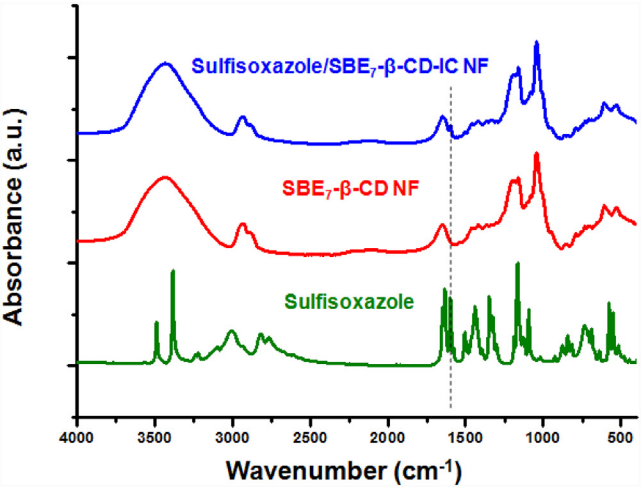

Fig. 8. FTIR spectra of sulfisoxazole, SBE_7-β-CD NF and sulfisoxazole/SBE_7-β-CD-IC NF.

remove undissolved sulfisoxazole. Then, absorbance versus wavelength plots of four samples was obtained from UV–vis spectroscopy (Varian, Cary 100). In addition, to show the fast-dissolving character and water-solubility enhancement of the drug visually, the water is directly added to solid sulfisoxazole, and sulfisoxazole/SBE_7-β-CD-IC NF and sulfisoxazole/SBE_7-β-CD-IC powder samples. The videos and pictures have been taken in which, sulfisoxazole powder and the sulfisoxazole/SBE_7-β-CD-IC NF were placed into petri dishes separately and then, 5 mL of water was added to petri dishes. Then, to make comparison sulfisoxazole/SBE_7-β-CD-IC powder were also placed into a petri dish and then, 5 mL of water was added.

3. Results and discussion

3.1. Phase solubility studies

Phase solubility diagram plotted by sulfisoxazole concentration versus SBE_7-β-CD concentration was given in Fig. 2 which corresponds that with increase in SBE_7-β-CD concentration, sulfisoxazole concentration also increases. The complex showed linear trend (A_L-type) demonstrating 1:1 complex formation tendency of sulfisoxazole and SBE_7-β-CD molecules. The stability constant (K_s) was calculated as 880 M^{-1} from the diagram according to Eqn. (1) and this value indicates better stability when compared to the previously done study on HPβCD by Gladys et al. (2003).

3.2. Electrospinning of SBE_7-β-CD NF and Sulfisoxazole/SBE_7-β-CD-IC NF

Since the phase solubility studies indicated 1:1 (sulfisoxazole: SBE_7-β-CD) complex formation tendency between sulfisoxazole and SBE_7-β-CD, first, we prepared 1:1 molar ratio inclusion complex between sulfisoxazole and SBE_7-β-CD by using highly concentrated SBE_7-β-CD (200% (w/v)) aqueous solution for the complexation. However, the electrospinning of uniform nanofibers from 1:1 molar ratio of sulfisoxazole/SBE_7-β-CD-IC system was not successful under the applied electrospinning conditions/parameters. Hence, we optimized the CD-IC solutions and found out that sulfisoxazole/SBE_7-β-CD-IC solution having 1:2 (sulfisoxazole: SBE_7-β-CD) molar ratio was more favorable for the electrospinning of uniform nanofibers. As a control sample, pristine SBE_7-β-CD NF was also electrospun and we obtained bead-free and uniform nanofiber morphology for the free-standing nanofibrous web of SBE_7-β-CD. The optimized parameters for the electrospinning of the bead-free nanofibers from pristine SBE_7-β-CD and sulfisoxazole/SBE_7-β-CD-IC systems were given in detail in experimental section. The photos of free-standing and flexible electrospun nanofibrous samples were given in Fig. 3a–b for pristine SBE_7-β-CD NF and sulfisoxazole/SBE_7-β-CD-IC NF. The representative SEM images of these SBE_7-β-CD NF and sulfisoxazole/SBE_7-β-CD-IC NF samples were given in Fig. 3c–d, respectively. From the SEM images, the average fiber diameter (AFD) for sulfisoxazole/SBE_7-β-CD-IC NF and pristine SBE_7-β-CD NF was calculated as 650 ± 290 nm and 890 ± 415 nm, respectively.

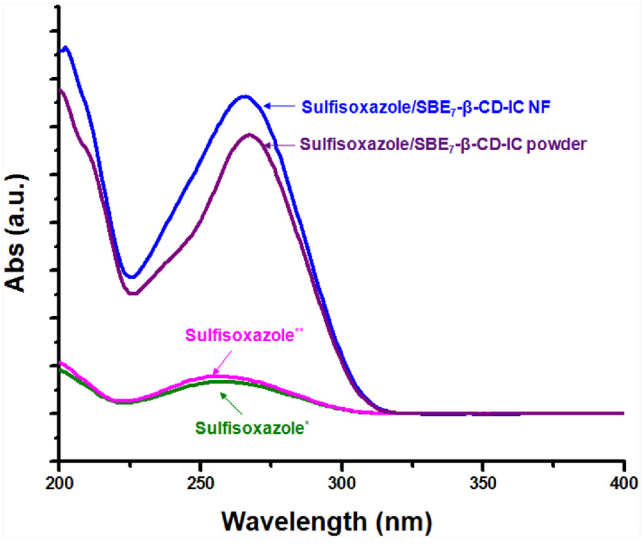

Fig. 9. Water solubility diagram of *sulfisoxazole with concentration of its water solubility (green), **excess amount of sulfisoxazole (pink), sulfisoxazole/SBE_7-β-CD-IC NF having the same excess amount of sulfisoxazole (blue), sulfisoxazole/SBE_7-β-CD-IC powder having the same excess amount of sulfisoxazole (purple). (For interpretation of the references to colour in this figure legend, the reader is referred to the web version of this article.)

3.3. Structural characterization of SBE_7-β-CD NF and Sulfisoxazole/SBE_7-β-CD-IC NF

The structural characterization of SBE_7-β-CD NF, sulfisoxazole/SBE_7-β-CD-IC NF and sulfisoxazole/SBE_7-β-CD-IC powder samples was done by using the different methods. ^{1}H NMR spectroscopy was used to obtain molar ratio of sulfisoxazole to SBE_7-β-CD in the sulfisoxazole/SBE_7-β-CD-IC NF matrix and sulfisoxazole/SBE_7-β-CD-IC powder. The ^{1}H NMR spectra of sulfisoxazole, SBE_7-β-CD powder, SBE_7-β-CD NF, sulfisoxazole/SBE_7-β-CD-IC NF and sulfisoxazole/SBE_7-β-CD-IC powder were evaluated (Fig. 4a–d). Protons of SBE_7-β-CD NF and as-received powder SBE_7-β-CD were appeared in the range of δ 1.5–5.8 ppm which is correlated with previous literature (Devasari et al., 2015; Kulkarni and Belgamwar, 2017). As shown in Fig. 4b, the ^{1}H NMR spectra of SBE_7-β-CD powder and SBE_7-β-CD NF present the same characteristic shifts which indicated that the electrospinning process did not cause any chemical degradation to the structure of SBE_7-β-CD. The molar ratio was calculated from integration of peak ratio between peak of sulfisoxazole at around 7.35 (H-a) and SBE_7-β-CD peak at around 5.00 ppm (H-1) as 0.28:1.00 for both sulfisoxazole/SBE_7-β-CD-IC NF and sulfisoxazole/SBE_7-β-CD-IC powder (Fig. 4c–d). This suggests that more than 50% (w/w) of initial sulfisoxazole amount was preserved for both nanofibrous web and powder form.

The thermal decomposition of sulfisoxazole, SBE_7-β-CD NF and sulfisoxazole/SBE_7-β-CD-IC NF were investigated by thermal gravimetric analysis (TGA) (Fig. 5). The weight losses below 100 °C belong to the water loss for all samples. Pure sulfisoxazole decomposition occured between 190- 400 °C while SBE_7-β-CD NF exhibited main degredation between 250 and 500 °C. Along with this, thermal decomposition of sulfisoxazole/SBE_7-β-CD-IC NF started at 220 °C and continued up to 500 °C. There are two differences between SBE_7-β-CD NF and sulfisoxazole/SBE_7-β-CD-IC NF degradation. First one is the small step starting at 220 °C which possibly belong to the sulfisoxazole. The shifting of thermal decomposition onset of sulfisoxazole from 190 °C to 220 °C showed the IC formation between sulfisoxazole and SBE_7-β-CD. The second difference is the intensity of peak at 300 °C which also proves the formation of inclusion complexes.

DSC is one of the widely used techniques to evaluate IC formation between CD and guest molecule in such a way that the melting point of guest molecules is not observed if guest molecules fully complexed within the CD cavities (Uyar et al., 2006). The DSC scans of pure sulfisoxazole, SBE_7-β-CD NF, sulfisoxazole/SBE_7-β-CD-IC NF and sulfisoxazole/SBE_7-β-CD-IC powder were given in Fig. 6. The pure sulfisoxazole DSC scan exhibited a melting point at

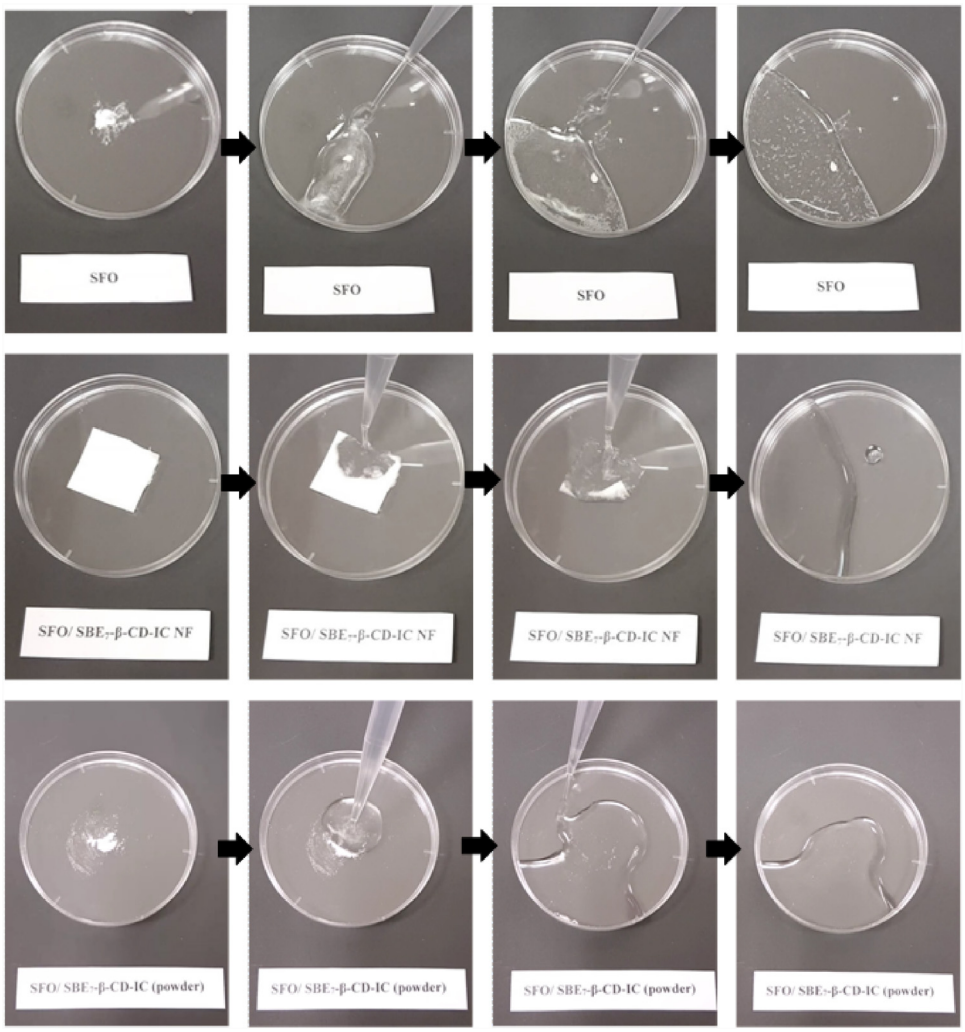

Fig. 10. Presentation of the solubility behaviour of sulfisoxazole (represented by "SFO"), sulfisoxazole/SBE_7-β-CD-IC NF and sulfisoxazole/SBE_7-β-CD-IC powder for a few seconds of water exposure. The pictures were captured from the videos which were given as Supporting information.

197 °C, whereas no melting point was observed for sulfisoxazole for the samples of sulfisoxazole/SBE_7-β-CD-IC NF and sulfisoxazole/SBE_7-β-CD-IC powder. The DSC results further confirm that the sulfisoxazole molecules are fully complexed with SBE_7-β-CD in the samples of sulfisoxazole/SBE_7-β-CD-IC NF and sulfisoxazole/SBE_7-β-CD-IC powder.

The crystalline structures of pure sulfisoxazole, SBE_7-β-CD NF, sulfisoxazole/SBE_7-β-CD-IC NF and sulfisoxazole/SBE_7-β-CD-IC powder were investigated by XRD to show the evidence of IC formation between sulfisoxazole and SBE_7-β-CD. Sulfisoxazole is a crystalline material having a sharp diffraction peaks at different 2θ values; however, the XRD pattern of SBE_7-β-CD NF, sulfisoxazole/SBE_7-β-CD-IC NF and sulfisoxazole/SBE_7-β-CD-IC powder are very similar which have amorphous structures. The sulfisoxazole/SBE_7-β-CD-IC NF and sulfisoxazole/SBE_7-β-CD-IC powder do not show any diffraction peaks of sulfisoxazole (Fig. 7). In other words, XRD results revealed the IC formation between sulfisoxazole and SBE_7-β-CD in the samples of sulfisoxazole/SBE_7-β-CD-IC NF and sulfisoxazole/SBE_7-β-CD-IC powder. The XRD result suggests that sulfisoxazole molecules are isolated from each other by entering into SBE_7-β-CD cavities and cannot form any crystalline aggregates. Since drugs in crystalline forms are more stable, their solubility decreases (Babu and Nangia, 2011); however, CD-IC formation prevent crystallization of drugs. Therefore, the solubility of sulfisoxazole increases by SBE_7-β-CD-IC formation since the crystallization of sulfisoxazole was prevented as confirmed by the XRD pattern.

The presence of guest molecule in structure and the formation of inclusion complexes between host and guest molecule can be proved by FTIR analysis. The FTIR spectra of pure sulfisoxazole, SBE_7-β-CD NF and sulfisoxazole/SBE_7-β-CD-IC NF are represented in Fig. 8. The FTIR spectrum of sulfisoxazole displayed salient peaks at 876–688 cm^{-1} range (C—H bending), at 1347 cm^{-1}, (SO_2 stretching); at 1326 cm^{-1} (aromatic ring stretching); at 1597 cm^{-1} (C=C stretching); at 1632 cm^{-1} (NH_2 deformation vibrations). The FTIR spectrum of SBE_7-β-CD showed a broad peak at between 3015 and 3760 cm^{-1} (O—H stretching vibration); a peak at 2931 cm^{-1} (C—H stretching vibrations); peaks at 1159 cm^{-1} and 1043 cm^{-1} (C—H and C—O stretching vibrations). Sulfisoxazole peaks were overlapped by CD peaks which makes the identification of each compounds complicated at the spectra of inclusion complex nanofibers. However, the sharpest absorption peak of sulfisoxazole at about 1597 cm^{-1} corresponding to C—H stretching vibration causes increase in intensity at that wavelength of inclusion complex nanofiber. This result suggested that sulfisoxazole is present in inclusion complex nanofibers.

3.4. Water-solubility of Sulfisoxazole/SBE_7-β-CD-IC NF

As mentioned Section 2.3, excess amount of sulfisoxazole (1.3 mg mL^{-1}) and sulfisoxazole/SBE_7-β-CD-IC NF and sulfisoxazole/SBE_7-β-CD-IC powder having the same amount of sulfisoxazole were added to water. In order to make comparison, the solution of sulfisoxazole with concentration of its water solubility (about 0.2 mg mL^{-1}) was also prepared to see water-solubility enhancement. The plot (Fig. 9) shows that the solutions of sulfisoxazole with 0.2 mg mL^{-1} concentration and of sulfisoxazole with 1.3 mg mL^{-1} demonstrated peak at almost the same absorbance. On the other hand, sulfisoxazole/SBE_7-β-CD-IC NF sample solution having 1.3 mg mL^{-1} of sulfisoxazole concentration showed peak at 10 times higher absorbance. This shows that the solubility of sulfisoxazole was increased by 10 times with sulfisoxazole/SBE_7-β-CD-IC NF formation. As seen from Fig. 9, sulfisoxazole/SBE_7-β-CD-IC powder also enhances water solubility of sulfisoxazole due to formation of CD-IC, however sulfisoxazole/SBE_7-β-CD-IC NF shows higher absorbance than sulfisoxazole/SBE_7-β-CD-IC powder. The high surface area to volume ratio, high porosity of nanofibers structure contribute to the enhancement of water solubility of the drug (Sebe et al., 2015); therefore, the water solubility enhancement in sulfisoxazole/SBE_7-β-CD-IC NF become higher compared to sulfisoxazole/SBE_7-β-CD-IC powder. The fast-dissolving property and water-solubility enhancement of the sulfisoxazole in sulfisoxazole/SBE_7-β-CD-IC NF and sulfisoxazole/SBE_7-β-CD-IC powder were also visually proven (Video S1, Video S2 and Fig. 10). After addition of 5 mL water to the petri dishes, while sulfisoxazole/SBE_7-β-CD-IC NF was dissolved immediately, the dissolution of sulfisoxazole/SBE_7-β-CD-IC powder took place a little bit slower than sulfisoxazole/SBE_7-β-CD-IC NF sample and the pure sulfisoxazole remain undissolved. This clearly showed the fast-dissolving property of sulfisoxazole/SBE_7-β-CD-IC NF along with highly-increased water-solubility of sulfisoxazole by sulfisoxazole/SBE_7-β-CD-IC NF formation.

4. Conclusions

In this study, free-standing and easily handled nanofibrous web of sulfisoxazole/SBE_7-β-CD-IC was successfully produced by using electrospinning technique. The electrospun sulfisoxazole/SBE_7-β-CD-IC nanofibrous web has shown the fast-dissolving property as well as the providing enhanced water-solubility to sulfisoxazole. Based on our results, it is concluded that SBE_7-β-CD is a good candidate to form ICs with sulfisoxazole to increase its water-solubility to a great extent. Moreover, electrospinning of nanofibers from sulfisoxazole/SBE_7-β-CD-IC system having high surface area to volume ratio and nano-scale porosity provides fast-dissolving property. In brief, electrospinning of nanofibers/nanowebs from drug/CD-ICs systems may provide novel approaches for enhanced water-solubility and fast-dissolving tablet formulations for drug delivery systems.

Acknowledgements

T. Uyar acknowledges The Turkish Academy of Sciences – Outstanding Young Scientists Award Program (TUBA-GEBIP)-Turkey for partial support of the research. Z. I. Yildiz thank to TUBITAK-BIDEB for the Ph.D. scholarship.

Appendix A. Supplementary data

Supplementary data associated with this article can be found, in the online version, at http://dx.doi.org/10.1016/j.ijpharm.2017.04.047.

References

Aytac, Z., Uyar, T., 2017. Core-shell nanofibers of curcumin/cyclodextrin inclusion complex and polylactic acid: enhanced water solubility and slow release of curcumin. Int. J. Pharm. 518, 177–184. doi:http://dx.doi.org/10.1016/j.ijpharm.2016.12.061.

Aytac, Z., Sen, H.S., Durgun, E., Uyar, T., 2015. Sulfisoxazole/cyclodextrin inclusion complex incorporated in electrospun hydroxypropyl cellulose nanofibers as drug delivery system. Colloids Surf. B: Biointerfaces 128, 331–338. doi:http://dx.doi.org/10.1016/j.colsurfb.2015.02.019.

Aytac, Z., Yildiz, Z.I., Kayaci-Senirmak, F., Keskin, N.O.S., Kusku, S.I., Durgun, E., Tekinay, T., Uyar, T., 2016a. Fast-Dissolving, prolonged release, and antibacterial cyclodextrin/Limonene-Inclusion complex nanofibrous webs via polymer-free electrospinning. J. Agric. Food Chem. 64, 7325–7334. doi:http://dx.doi.org/10.1021/acs.jafc.6b02632.

Aytac, Z., Yildiz, Z.I., Kayaci-Senirmak, F., Keskin, N.O.S., Tekinay, T., Uyar, T., 2016b. Electrospinning of polymer-free cyclodextrin/geraniol–inclusion complex nanofibers: enhanced shelf-life of geraniol with antibacterial and antioxidant properties. RSC Adv. 6, 46089–46099. doi:http://dx.doi.org/10.1039/c6ra07088d.

Aytac, Z., Keskin, N.O.S., Tekinay, T., Uyar, T., 2017. Antioxidant α-tocopherol/γ-cyclodextrin-inclusion complex encapsulated poly(lactic acid) electrospun nanofibrous web for food packaging. J. Appl. Polym. Sci. 134 (21) doi:http://dx.doi.org/10.1002/app.44858.

Babu, N.J., Nangia, A., 2011. Solubility advantage of amorphous drugs and pharmaceutical cocrystals. Cryst. Growth Des. 11, 2662–2679. doi:http://dx.doi.org/10.1021/cg200492w.

Beig, A., Agbaria, R., Dahan, A., 2015. The use of captisol (SBE_7-β-CD) in oral solubility-enabling formulations: comparison to HPβCD and the solubility–permeability interplay. Eur. J. Pharm. Sci. 77, 73–78. doi:http://dx.doi.org/10.1016/j.ejps.2015.05.024.

Celebioglu, A., Uyar, T., 2011. Electrospinning of polymer-free nanofibers from cyclodextrin inclusion complexes. Langmuir 27, 6218–6226. doi:http://dx.doi.org/10.1021/la1050223.

Celebioglu, A., Uyar, T., 2012. Electrospinning of nanofibers from non-polymeric systems: polymer-free nanofibers from cyclodextrin derivatives. Nanoscale 4, 621–631. doi:http://dx.doi.org/10.1039/c1nr11364j.

Celebioglu, A., Uyar, T., 2013. Electrospinning of nanofibers from non-polymeric systems: electrospun nanofibers from native cyclodextrins. J. Colloid Interface Sci. 404, 1–7. doi:http://dx.doi.org/10.1016/j.jcis.2013.04.034.

Celebioglu, A., Umu, O.C., Tekinay, T., Uyar, T., 2014a. Antibacterial electrospun nanofibers from triclosan/cyclodextrin inclusion complexes. Colloids Surf. B: Biointerfaces 116, 612–619. doi:http://dx.doi.org/10.1016/j.colsurfb.2013.10.029.

Celebioglu, A., Vempati, S., Ozgit-Akgun, C., Biyikli, N., Uyar, T., 2014b. Water-soluble non-polymeric electrospun cyclodextrin nanofiber template for the synthesis of metal oxide tubes by atomic layer deposition. RSC Adv. 4, 61698–61705. doi:http://dx.doi.org/10.1039/c4ra12073f.

Celebioglu, A., Kayaci-Senirmak, F., Ipek, S., Durgun, E., Uyar, T., 2016. Polymer-free nanofibers from vanillin/cyclodextrin inclusion complexes: high thermal stability, enhanced solubility and antioxidant property. Food Funct. 7, 3141–3153. doi:http://dx.doi.org/10.1039/c6fo00569a.

Devasari, N., Dora, C.P., Singh, C., Paidi, S.R., Kumar, V., Sobhia, M.E., Suresh, S., 2015. Inclusion complex of erlotinib with sulfobutyl ether-β-cyclodextrin: preparation, characterization, in silico, in vitro and in vivo evaluation. Carbohydr. Polym. 134, 547–556. doi:http://dx.doi.org/10.1016/j.carbpol.2015.08.012.

Gladys, G., Claudia, G., Marcela, L., 2003. The effect of pH and triethanolamine on sulfisoxazole complexation with hydroxypropyl-β-cyclodextrin. Eur. J. Pharm. Sci. 20, 285–293. doi:http://dx.doi.org/10.1016/s0928-0987(03)00202-1.

Higuchi, T., Connors, A.K., 1965. Phase-solubility techniques. Adv. Anal. Chemistry and Instrum. 4, 117–212.

Kulkarni, A.D., Belgamwar, V.S., 2017. Inclusion complex of chrysin with sulfobutyl ether-β-cyclodextrin (Captisol®): Preparation, characterization, molecular modelling and in vitro anticancer activity. J. Mol. Struct. 1128, 563–571. doi:http://dx.doi.org/10.1016/j.molstruc.2016.09.025.

Mendes, A.C., Gorzelanny, C., Halter, N., Schneider, S.W., Chronakis, I.S., 2016. Hybrid electrospun chitosan-phospholipids nanofibers for transdermal drug delivery. Int. J. Pharm. 510, 48–56. doi:http://dx.doi.org/10.1016/j.ijpharm.2016.06.016.

Noruzi, M., 2016. Electrospun nanofibres in agriculture and the food industry: a review. J. Sci. Food Agric. 96, 4663–4678. doi:http://dx.doi.org/10.1002/jsfa.7737.

Ogawa, N., Takahashi, C., Yamamoto, H., 2015. Physicochemical characterization of cyclodextrin–drug interactions in the solid state and the effect of water on these interactions. J. Pharm. Sci. 104, 942–954. doi:http://dx.doi.org/10.1002/jps.24319.

Sahay, R., Kumar, P.S., Sridhar, R., Sundaramurthy, J., Venugopal, J., Mhaisalkar, S.G., Ramakrishna, S., 2012. Electrospun composite nanofibers and their multifaceted applications. J. Mater. Chem. 22, 12953. doi:http://dx.doi.org/10.1039/c2jm30966a.

Sebe, I., Szabó, P., Kállai-Szabó, B., Zelkó, R., 2015. Incorporating small molecules or biologics into nanofibers for optimized drug release: a review. Int. J. Pharm. 494 (1), 516–530.

Siafaka, P., Okur, N.Ü., Mone, M., Giannakopoulou, S., Er, S., Pavlidou, E., Karavas, E., Bikiaris, D., 2016. Two different approaches for oral administration of

voriconazole loaded formulations: electrospun fibers versus β-Cyclodextrin complexes. Int. J. Mol. Sci. 17, 282. doi:http://dx.doi.org/10.3390/ijms17030282.
Szejtli, J., 1998. Introduction and general overview of cyclodextrin chemistry. Chem. Rev. 98, 1743–1754. doi:http://dx.doi.org/10.1021/cr970022c.
Tačić, A., Savić, I., Nikolić, V., Savić, I., Ilić-Stojanović, S., Ilić, D., Petrović, S., Popsavin, M., Kapor, A., 2014. Inclusion complexes of sulfanilamide with β-cyclodextrin and 2-hydroxypropyl-(-cyclodextrin. J. Inclusion Phenom. Macrocyclic Chem. 80, 113–124. doi:http://dx.doi.org/10.1007/s10847-014-0410-x.
Tonglairoum, P., Chuchote, T., Ngawhirunpat, T., Rojanarata, T., Opanasopit, P., 2013. Encapsulation of plai oil/2-hydroxypropyl-β-cyclodextrin inclusion complexes in polyvinylpyrrolidone (PVP) electrospun nanofibers for topical application. Pharm. Dev. Technol. 19, 430–437. doi:http://dx.doi.org/10.3109/10837450.2013.788659.
Uyar, T., Kny, E., 2017. Electrospun Materials for Tissue Engineering and Biomedical Applications, first ed. Elsevier, Woodhead Publishing (ISBN: 9780081010228).
Uyar, T., El-Shafei, A., Wang, X., Hacaloglu, J., Tonelli, A.E., 2006. The solid channel structure inclusion complex formed between guest styrene and host γ-cyclodextrin. J. Inclusion Phenom. Macrocyclic Chem. 55 (1), 109–121. doi:http://dx.doi.org/10.1007/s10847-005-9026-5.
Wang, B., Li, H., Yao, Q., Zhang, Y., Zhu, X., Xia, T., Wang, J., Li, G., Li, X., Ni, S., 2016. Local in vitro delivery of rapamycin from electrospun PEO/PDLLA nanofibers for glioblastoma treatment. Biomed. Pharmacother. 83, 1345–1352. doi:http://dx.doi.org/10.1016/j.biopha.2016.08.033.
Wendorff, J.H., Agarwal, S., Greiner, A., 2012. Electrospinning: Materials, Processing, and Applications. Wiley-VCH, Weinheim, Germany.